www.czasopisma.pan.pl PAN www.journals.pan.pl

GEODESY AND CARTOGRAPHY
Vol. 67, No. 2, 2018, pp. 321–343

DOI: https://doi.org/10.24425/118706

Original research paper

2D Cadastral Coordinate Transformation using extreme learning machine technique

Yao Yevenyo Ziggah[1*], Yakubu Issaka[2], Prosper Basommi Laari[3], Zhenyang Hui[4]

[1,2]University of Mines and Technology
Faculty of Mineral Resources Technology, Department of Geomatic Engineering
Tarkwa-Esiama Rd, Tarkwa, Ghana
[1]e-mail: yyziggah@umat.edu.gh, ORCID: http://orcid.org/0000-0002-9940-1845
[2]e-mail: yissaka@umat.edu.gh, ORCID: http://orcid.org/0000-0002-5027-0776

[3]University for Development Studies
Department of Environment and Resource Studies, Central Administration Doungou
Kumasi Rd, Wa, Ghana
e-mail: einsteinpd2002@yahoo.com, ORCID: http://orcid.org/0000-0002-3209-1408

[4]East China University of Technology, Faculty of Geomatics
Nanchang 330013, P. R. China
e-mail: huizhenyang2008@163.com, ORCID: http://orcid.org/0000-0002-1377-2558

[*]Corresponding author: Yao Yevenyo Ziggah

Received: 10 May 2018 / Accepted: 3 September 2018

Abstract: Land surveyors, photogrammetrists, remote sensing engineers and professionals in the Earth sciences are often faced with the task of transferring coordinates from one geodetic datum into another to serve their desired purpose. The essence is to create compatibility between data related to different geodetic reference frames for geospatial applications. Strictly speaking, conventional techniques of conformal, affine and projective transformation models are mostly used to accomplish such task. With developing countries like Ghana where there is no immediate plans to establish geocentric datum and still rely on the astro-geodetic datums as it national mapping reference surface, there is the urgent need to explore the suitability of other transformation methods. In this study, an effort has been made to explore the proficiency of the Extreme Learning Machine (ELM) as a novel alternative coordinate transformation method. The proposed ELM approach was applied to data found in the Ghana geodetic reference network. The ELM transformation result has been analysed and compared with benchmark methods of backpropagation neural network (BPNN), radial basis function neural network (RBFNN), two-dimensional (2D) affine and 2D conformal. The overall study results indicate that the ELM can produce comparable transformation results to the widely used BPNN and RBFNN, but better than the 2D affine and 2D conformal. The results produced by ELM has demonstrated it as a promising tool for coordinate transformation in Ghana.

Keywords: coordinate transformation, extreme learning machine, backpropagation neural network, radial basis function neural network, geodetic datum

1. Introduction

Unifying data related to different geodetic datums is a geodetically sensitive means to create data compatibility and to reduce potential errors due to different datums position, size and shape. This data unification is usually accomplished through the process of coordinate transformation. This transformation is highly significant to Earth resource professionals because natural and man-made features are usually represented geographically by positional information. For example, exploration and extraction of natural resources such as gold, bauxite, manganese, diamond, oil and natural gas require the use of coordinates to identify their locations. Therefore, it is quite clear that accurate positional information should be provided for proper planning, management and decision making. Hence, the essence of performing coordinate transformation is to help integrate data obtained in the national and global coordinate systems (Konakoğlu and Gökalp, 2016) thereby enabling Earth resource professionals to accurately use coordinates required in a specific datum.

So far, various techniques have been reported in the literature for performing coordinate transformation in both 2D and 3D, respectively. The present study is focussed on the 2D coordinate transformation since the coordinate system used in Ghana for surveying and mapping purposes is a 2D projected grid coordinate (Easting, Northing) based on the Transverse Mercator 1° NW (Ayer and Fosu, 2008; Mugnier, 2000). Moreover, the two local geodetic datums namely Accra 1929 and Leigon 1977 are being used concurrently for geodetic tasks even though the Accra 1929 datum is the official system of reference recommended by the Ghana Survey and Mapping Division (Ayer and Fosu, 2008). Hence, the field practitioners in Ghana are required to transform the Leigon 1977 datum coordinates into the Accra 1929 datum. Furthermore, with Ghana having no immediate plans to establish geocentric datum and still rely on the two aforementioned astro-geodetic datums for its surveying and mapping activities, there is the pressing need to assess the capability of other coordinate transformation procedures. These assertions made here have also been opined by several researchers in Ghana (Poku-Gyamfi, 2009; Dzidefo, 2011; Kotzev, 2013). It is therefore necessary to apply and test the potential of alternative methods applicable to transform 2D coordinates between the Accra 1929 and Legion 1977 datums in Ghana.

Generally, in the 2D coordinate transformation, three conventional techniques are usually applied. These are conformal, affine and projective transformation models, respectively (Ghilani, 2010). Several studies have been carried out regarding the efficiency of these classical methods. Authors, for example, Al-Ruzouq and Dimitrova (2006) evaluated the performance of 2D-conformal, affine and projective techniques for merging mismatched old cadastral maps prepared at different scales in the early thirties and current ground truths by determining transformation parameters for cadastral mapping in Jordan. Here, the transformation techniques were applied to match coordinates from IKONOS satellite image and scanned cadastral maps with orthophoto points. The applicability of the transformation techniques to different relief was also tested. It was proposed that in flat areas the 2D affine model was better, while the 2D projective model was more appropriate for hilly areas. The 2D conformal model, on the other

hand, was recommended for less demanding accuracy geodetic applications in Jordan. Deakin (2007) provided the theoretical basis and application of 2D conformal model for cadastral surveying purposes and determination of the transformation parameters using least squares adjustment technique. The successes of 2D affine model applied to ordinary least squares, least absolute value and total least squares procedures have also been demonstrated in Sisman (2014). The essence of the study was to apply different adjustment procedures to the 2D affine model for transforming the analogue cadastral maps produced in 1990 using the conventional surveying technique for the Samsun Province into the Turkish national coordinate system. The presented analyses in Sisman (2014) revealed that the ordinary least squares method was more appropriate if the data points is free from blunders and systematic errors. However, for the determination of erroneous measurements, the author suggested that the least absolute value must first be applied before using the least squares method. In Fotiou and Kaltsikis (2016), a modified mixed model based on the Gauss Helmert model of the 2D conformal model was presented. It was observed that the use of the modified mixed model is useful in instances where the co-located points have different precision. With regards to equal observation precision, the modified mixed model and Gauss Helmert model provided identical transformation results as those of the traditional Gaussian mixture model. Elsewhere, conversion of the physical constraints into mathematical notations and to use constrained total least squares to solve the problem of 2D affine transformation has been presented (Zhang et al., 2016). In Dönmez and Tunc (2016), the 2D conformal and first order polynomial model was applied to transform orthophoto and cadastral map of the Kagithane District in Istanbul, Turkey. The results revealed that both transformation methods produced reliable and accurate transformed coordinate values. Based on the results obtained, Dönmez and Tunc (2016) concluded that cadastral maps could be used as base maps for aerial orthophotos. It is quite logical to state here that the use of the conventional 2D coordinate transformation techniques for geodetic applications is still an on-going research in geodetic sciences.

In the last few years, several soft computing methods have been used as alternative to the aforementioned conventional techniques to perform coordinate transformation. Of particular significance to mention, the artificial neural network (ANN) algorithms have been accepted as a reliable tool for research due its function approximation, clustering and pattern recognition abilities. Generally, ANN has been the most widely used methods for both 2D and 3D coordinate transformation. The reason is that several authors have extensively investigated the capability and applicability of the radial basis function neural network (RBFNN) as alternative to the traditional methods. Their obtained results have been compared to the conventional methods such as the three-parameter, standard Molodensky equation, Bursa-Wolf, Molodensky-Badekas, 2D conformal model and 2D Affine, respectively (Barsi, 2001; Tierra et al., 2008, 2009; Gullu, 2010; Gullu et al., 2011; Konakoğlu et al., 2016). Similarly, the back propagation neural network (BPNN) has also been tested and compared in the same fashion (Zaletnyik, 2004; Lao-Sheng and Yi-Jin, 2006; Turgut, 2010; Yilmaz and Gullu, 2012; Mihalache, 2012; Tierra and Romero, 2014; Konakoğlu et al., 2016; Konakoğlu and Gökalp, 2016). The general conclusions gathered from these studies indicate that the RBFNN and BPNN calibrated

correctly on the model construction dataset (training) and predicted the test coordinates with better accuracy than the conventional transformation methods. The supervised training of the RBFNN and BPNN was carried out in those studies using co-located points in both the input and output systems. It was demonstrated that using the ANN eliminate the estimation of transformation parameters because a single training was enough for developing ANN transformation model. Therefore, a well-structured ANN would produce results that could be used for practical surveying and mapping purposes.

It must be acknowledged that an investigation into a genetic-based method using symbolic regression for directly transforming GPS coordinates to 2D coordinates has also been studied (Wu et al., 2008). The proposed approach could statistically reduce inaccuracy associated with data related to the local reference ellipsoid as well as the GPS coordinates used. However, a major shortcoming of the genetic-based approach is slow convergence in the training phase even though the coordinates could be calculated straightforwardly once a regression formula is formed. In addition, re-training is required when new untrained data are introduced for a new area. This phenomenon has been attributed to the fact that the genetic-based approach does not support incremental regression. A preliminary study on the concept of the neuro-fuzzy neural network based on the Takagi-Sugeno-Kang system for coordinate transformation has also been explored of which encouraging results have been reported (Gil and Mrówczyńska, 2012). Recently, ElSayed and Ali (2016) applied fuzzy multiple linear regression to assess its effect on total least squares and ordinary least squares in coordinate transformation process. The authors considered the weighted and unweighted conditions of applying the least squares methods. Improved transformation result was reported with the fuzzy approach which eliminates the need to accurately assign weight and confidence to the data.

From the above, it is obvious that soft computing algorithms have situated themselves as one of the present and most proficient methods that can be utilized as alternatives to other coordinate transformation methods. Although ANN techniques have extensively and successfully been utilised in coordinate transformation, the methods exhibit some practical drawbacks. Firstly, because ANN uses the gradient-based algorithms, the speed of learning is generally slower and thus computationally expensive (Huang et al., 2006a). Moreover, the ANN require setting up of several training parameters that are iteratively tuned which sometimes may result in converging in local minima rather than global minima (Huang et al., 2006a). As a means to overcome these defects, this study applied the extreme learning machine (ELM), which is a moderately new learning paradigm introduced by Huang et al. (2006b) for single-hidden-layer feedforward neural network. It must be noted that the ELM system process information in the hidden layer and the hidden nodes are the neurons found in the hidden layer.

ELM has been shown to offer some advantages over the ANN in terms of higher computational speed, global optimum realisation, good generalisation performance and less manual interference in the model formulation process (Huang and Babri, 1998; Huang et al., 2006b, 2015). It is noteworthy that the ELM have found applications in a number of geoscientific domains not limited to, landslide studies (Lian et al., 2014; Huang et al., 2017), change detection (Pal, 2009; Chang et al., 2010), meteorological

studies (Mohammadi, 2015; Lazarevska, 2016), Earth orientation parameters estimation (Lei et al., 2015) and hydrological studies (Tiwari et al., 2016; Deo and Sahin, 2016; Deo et al., 2017).

In spite of the fact that several scholars have applied the ELM model in recent years, performing coordinate transformation using this new robust technique to offer increased accuracy and reliability have not been captured in the literature. In line with that, the present study applied the ELM algorithm for the first time to perform coordinate transformation. The main objective of this study is to investigate the viability of utilising an ELM algorithm in coordinate transformation. Moreover, it is aimed at exploiting the merits of this method to perform cadastral coordinate transformation from the Leigon 1977 datum to the official Accra 1929 datum as a case study in Ghana geodetic reference network. Recent studies in Ghana have shown that the benchmarks methods of BPNN and RBFNN have been applied to carry out coordinate transformation between Accra 1929 and Leigon 1977 datums (Ziggah et al., 2016; Kumi-Boateng and Ziggah, 2017). Therefore, to ascertain the proficiency of the ELM in this study, its resulting performance was compared with the BPNN, RBFNN and two classical transformation methods (2D affine and 2D conformal). Usage of the proposed ELM approach could meet the accuracy standards required for cadastral applications in Ghana. Additionally, the results presented in this study have shown that ELM is very useful and can be an outstanding supplement to other cadastral coordinate transformation methods utilised in Ghana.

In the next section, the study area and data utilised are described. Section 3 briefly presents the theoretical concept of the methods applied and how the models were formulated. Section 4 gives the statistical performance indicators used to evaluate the results produced by the various methods, while Section 5 discusses the results. The study ends with conclusions in Section 6, respectively.

2. Study area and data description

The entire study was focused on the Ghana geodetic reference network (Figure 1). Ghana is a West African country that shares border in the West with Ivory Coast, Togo to the East, Burkina Faso to the North and Gulf of Guinea to the South. Its total land area is approximately 238,540 km^2 (Fosu et al., 2006) and lies between latitudes 4° 30′ N and 11° N, and between longitudes 3° W and 1° E, respectively (Mugnier, 2000).

Two national horizontal geodetic datums, the Accra datum 1929 and Leigon datum 1977 are being utilised concurrently by geodetic practitioners in Ghana (Ayer and Fosu, 2008; Mugnier, 2000; Poku-Gyamfi, 2009). The Accra 1929 datum is the local realisation of the War Office 1926 ellipsoid, while the Leigon 1977 datum is the realisation of the Clark 1880 (modified) ellipsoid (Ayer and Fosu, 2008; Ayer, 2008). The ellipsoid properties of the War Office 1926 include semi-major axis (a) = 6378299.99899832 m and semi-minor axis (b) = 6356751.68824042 m. However, the Clark 1880 (modified) has the semi-major axis (a) = 6378249.145 m and semi-minor axis (b) = 6356514.870 m. The Ghana national mapping coordinate system is a 2D projected grid coordinates of Easting and Northing based on the Transverse Mercator

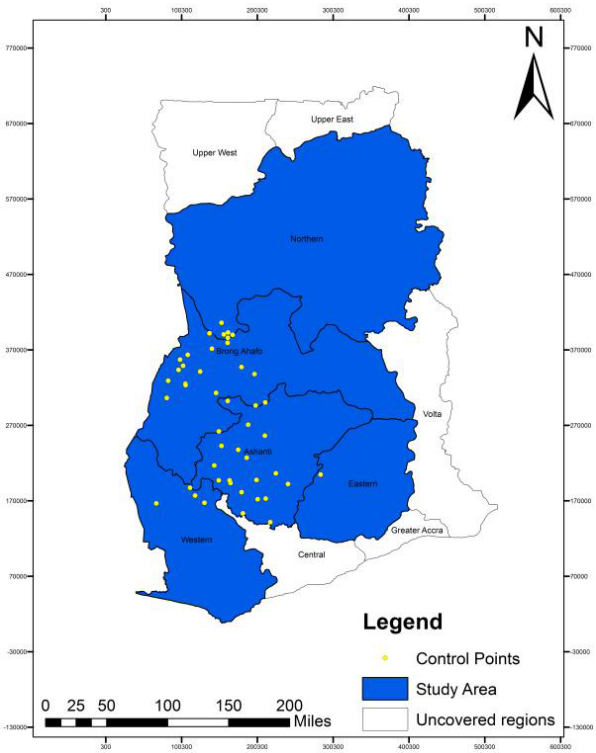

Fig. 1. Study Area: distribution of data points

1° NW. That is, Ghana's adopted Transverse Mercator projection has longitude 1° 00′ W as its central meridian having latitude 4° 40′ N. In order to avoid negative coordinates, 274319.736 m has been added to all Y coordinates that served as the false Easting, while the false Northing has been set to zero. A scale factor of 0.99975 is used at the central meridian so that the scale distortion exceeds the projection values only at the extreme ends of the country (Mugnier, 2000).

In the present study, 46 co-located control points (Figure 1) in projected grid coordinates for the Accra 1929 and Leigon 1977 datums have been provided by the Ghana Survey and Mapping Division of Lands Commission from the on-going Land Administration Project funded by the World Bank. These dataset constitute the national local coordinates of the on-going nationwide Global Positioning System (GPS) reference network establishment. The area coverage (five regions) of the 46 co-located control points (Figure 1) constitute the completed first phase of the Land Administration Project.

3. Methods

The following sections give a brief account on the theoretical concepts of the various techniques applied in this study.

3.1. Extreme learning machine

ELM introduced by Huang et al. (2006a) is a new training algorithm for single-hidden-layer feedforward neural network (SLFN) that can be applied to solve pattern recognition, clustering and function estimation related problems. This algorithm has the ability to randomly select the hidden and input layer neurons connecting weights as well as the biases of the hidden layer based on the condition that the hidden layer activation function is infinitely differentiable. Unlike the backpropagation learning algorithm, the randomly assigned weights and biases in the ELM remain the same during the training process. Moreover, in the ELM model development process only the number of hidden layer neurons is needed to be set by the modeller. Hence, the ELM algorithm trains ten times faster than the backpropagation neural network (Huang et al., 2006; Zhang et al., 2013; Deo and Sahin, 2016).

Given a set of training examples $D = \{(x_i, y_j) \mid i = 1, 2, \ldots, n\}$ with input data $x_i = [x_{i1}, \ldots, x_{in}]^T \in R^n$ and expected output values $y_j = [y_{j1}, \ldots, y_{jm}]^T \in R^m$, where R^n is the n-dimensional vector space and R^m one-dimensional output vector space. If the SLFN can successfully approximate the training samples D with zero error, then the output y_j of the ELM for the generalised SLFN can be expressed mathematically in Eq. (1) as

$$y_j = \sum_{i=1}^{Q} \beta_i g(w_i, b_i, x_j), \qquad j = 1, \ldots, n, \tag{1}$$

where Q denotes the hidden layer nodes, $g(x)$ is the activation function, w_i is the interconnecting weight between the i-th hidden node and the input nodes. b_i indicate the bias associated with the i-th hidden node and β_i is the weight vector connecting the i-th hidden node and the output node. Representing Eq. (1) in a compact form will give Eq. (2).

$$H\beta = Y, \tag{2}$$

where H is the output matrix of the hidden layer, β (defined in Eq. (1)) and Y is the desired target matrix of the training data. The mathematical notations for H, β and Y are given by Eqs. (3), (4) and (5), respectively. It should be noted that the i-th column of the H matrix (Eq. (3)) is the i-th output of the hidden node that matches the inputs x_1, x_2, x_3, …, x_n.

$$H(w_1, \ldots, w_L,\ b_i, \ldots, b_L,\ x_1, \ldots, x_n) = \begin{bmatrix} g(w_1, b_1, x_1) & \ldots & g(w_L, b_L, x_1) \\ \vdots & \ldots & \vdots \\ g(w_1, b_1, x_n) & \ldots & g(w_L, b_L, x_n) \end{bmatrix}_{n \times L}, \tag{3}$$

$$\beta = \begin{bmatrix} \beta_1^T \\ \vdots \\ \beta_L^T \end{bmatrix}_{L \times m}, \tag{4}$$

$$Y = \begin{bmatrix} y_1^T \\ \vdots \\ y_n^T \end{bmatrix}_{n \times m} . \tag{5}$$

Consequently, training the SLFN becomes computing the output weights $\hat{\beta}$ connecting the hidden layer to the output layer by finding the minimum norm least squares solution of Eq. (2). Hence, Eq. (2) becomes Eq. (6) for $\hat{\beta}$.

$$\hat{\beta} = H^{+}Y. \tag{6}$$

Here, H^{+} denotes Moore-Penrose generalised inverse of the hidden layer output matrix H and $Y = [y_1, \ldots, y_n]^T$.

The procedural framework of the ELM algorithm can be summarised as follows:

i. Input weights w_i and hidden layer threshold b_i should be randomly assigned based on the input data, activation function and number of hidden neurons.
ii. Compute the output matrix H for the hidden layer.
iii. Determine the output layer weight $\hat{\beta}$ expressed in Eq. (6).

3.2. Back propagation neural network

The present study applied the most widely used supervised BPNN which allows for the iterative fine-tuning of weights to improve the prediction accuracy of a model (Rumelhart et al., 1986). The BPNN, as utilised in this study, is a three-layered network (Figure 2) where $(X_1, X_2, X_3, \ldots, X_i)$ and $(Y_1, Y_2, Y_3, \ldots, Y_K)$ are the input and target training examples.

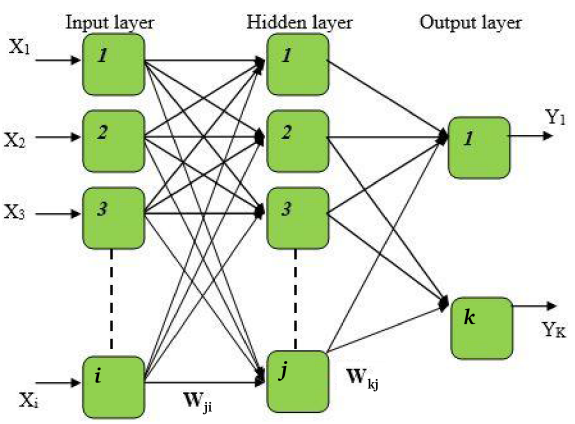

Fig. 2. BPNN architecture

Based on the theoretical work of Hornik et al. (1986), defining one hidden layer is enough to proficiently approximate any discrete and continuous nonlinear function with the desired accuracy. Therefore, the present study applied one hidden layer in the

BPNN structure. The optimum number of hidden neurons was determined by sequential trial and error procedure by monitoring the training and testing stages mean squared error values and making sound judgments. These hidden neurons allow the network to capture the pattern in the data and map the nonlinearity between input and output data sets (Swadi, 2010).

The computational procedures of the BPNN model are described as follows. First, the training input data $(X_1, X_2, X_3, \ldots, X_i)$ is received from the external environment by the input layer. This is then sent directly into the network through the hidden layer nodes. In the hidden layer, the inputs data are multiplied by their respective weights and summed together with a bias C. Equation (7) illustrates the calculation process in the hidden layer node j.

$$network_j = C_j + \sum W_{ji} X_i, \qquad i = 1,2,\ldots,m, \quad j = 1,2,\ldots,s, \tag{7}$$

where X_i represents the input data of the unit i, W_{ji} is the weight connecting the input layer unit i to the hidden unit j. The output of the hidden layer unit j denoted as H_j is given by Eq. (8).

$$H_j = tf(network_j), \tag{8}$$

where tf denote the transfer function. This study applied the hyperbolic tangent transfer function (Eq. (9)) (Yonaba et al., 2010) in the hidden layer.

$$f(x) = \tanh(x) = \frac{2}{1+e^{-2x}} - 1. \tag{9}$$

The output layer then receives the outputs of the hidden layer units H_j as its input. Here, the output layer computes the $network_h$ given by Eq. (10) as

$$network_h = C_h + \sum \alpha_{hj} H_j, \qquad j = 1,\ 2,\ \ldots, s, \quad h = 1, \tag{10}$$

where $network_h$ is the network value for the output unit h, α_{hj} is the weight linking the hidden unit j to the output unit h and H_j is the output of the hidden unit j, which is input for the output unit h. The output unit then applies a transfer function f to the $network_h$. The linear transfer function was used in the output layer. The output layer unit h results can be defined in Eq. (11) as

$$Y_h = f\left(C_h + \sum \alpha_{hj} G\left(C_j + \sum W_{ji} X_i\right)\right). \tag{11}$$

If the forecasted results from Eq. (11) differ from the expected outputs, an error is computed and reverted through the network from the output layer to the input layer. The main objective is to minimize the prediction error by changing the connection weights (W and α) (Eq. (11)) using a learning rule. It is worth mentioning that during the learning phase the bias input for the hidden and output layer neurons is adjusted like the other weights values. Due to the slowness to reach convergence, coupled with inefficiency and lack of robustness by the gradient descent algorithm when training a multilayer network, several authors have resorted to the Levenberg–Marquardt algorithm

(Zounemat-Kermani, 2012; Afzali, 2012). This is because the Levenberg–Marquardt algorithm has the capability to overcome the shortcomings of the gradient descent method. Hence, this study applied the Levenberg–Marquardt algorithm in the multilayer network. This algorithm can be viewed as a combination of steepest descent algorithm and the Gauss–Newton optimization technique (Hao and Wilamowski, 2011). Its mathematical representation is given in Eq. (12).

$$L = J^T J + VI, \tag{12}$$

where: J is the Jacobian matrix containing the derivatives of each error to each weight, V is a scalar called the combination coefficient and I is the identity matrix. The update rule of Levenberg–Marquardt algorithm can be defined in Eq. (13) as:

$$\Delta W = \left(J^T J + VI\right)^{-1} JE, \tag{13}$$

where: E is an error vector. In the course of the training process, the Levenberg–Marquardt algorithm switches between the steepest descent algorithm and the Gauss–Newton algorithm. When the scalar value V is close to zero or small, Eq. (13) approaches the update rule of the Gauss–Newton algorithm (Hao and Wilamowski, 2011) written in Eq. (14) as

$$\Delta W = \left(J^T J\right)^{-1} JE. \tag{14}$$

In contrast, when the scalar value V is very large, Eq. (13) approximate to the steepest descent algorithm given by Eq. (15).

$$\Delta w = \beta g, \tag{15}$$

where β is the learning constant and g being the gradient expressed in Eq. (16).

$$g = \frac{\partial E(X,w)}{\partial w} = \left[\frac{\partial E}{\partial w_1}\frac{\partial E}{\partial w_2}\cdots\frac{\partial E}{\partial w_N}\right]^T. \tag{16}$$

The network will stop the iteration process when there is no further improvement in the estimated errors.

3.3. Radial basis function neural network

RBFNN is a feed-forward network that utilises the supervised learning technique for solving function approximation and classification related problems (Broomhead and Lowe, 1988; Marwala, 2013). The network is made up of input, hidden and output layers which are directly connected together. The input and output units comprise of the explanatory and predicted response variable. The RBFNN uses a single hidden layer which applies the radial basis transfer function to approximate the training data in a high-dimensional space with some precision (Aharkava, 2010). Figure 3 depicts a simple RBFNN architecture of inputs $(X_1, X_2, X_3, \ldots, X_N)$, radial basis functions $(\phi_1, \phi_2, \ldots, \phi_M)$, weights $(W_1, W_2, \ldots, W_N)$ and output (Y), respectively.

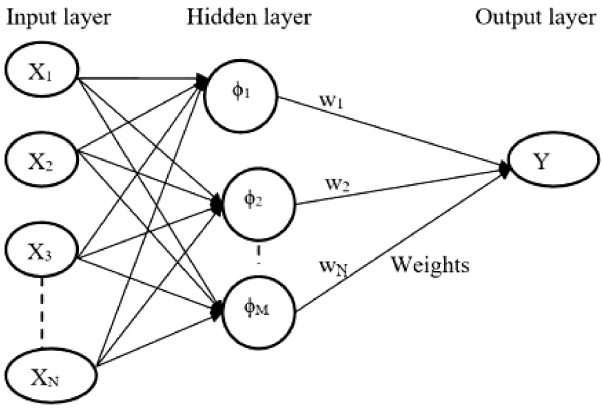

Fig. 3. RBFNN scheme

Given a set of input vector $X = \{x_1, x_2, \ldots, x_N\} \in R^N$ and corresponding output $Y = \{y_1, y_2, \ldots, y_k\} \in R$, the RBFNN task is to produce a function say $g(x)$ that can sufficiently map the input–output relationship of the dataset. The RBFNN model (Bishop, 1995; Marwala, 2013) has been represented mathematically in Eq. (17).

$$y_k = g_k(x) = \sum_{j=1}^{M} w_{jk}\phi_j(x), \qquad k = 1,2,3,\ldots,M. \tag{17}$$

Here, $y_k \in R$ is the predicted outcome of the network based on X (input vectors), M represents the total number of hidden neurons, w_{jk} are the output weights corresponding to the link between a hidden node and an output node, $\phi_j(.)$ is the j-th nonlinear transfer function. The number of hidden layer neurons in the RBFNN corresponds to the number of radial basis function (RBF) applied during the training phase of the network. It is therefore essential to select an adequate number of RBFs such that the centres of these basis functions can correctly map the surface of the input space (Yih-Jiuan, 1998). The present study chose and implemented the Gaussian activation function (Eq. (18)) in the hidden layer chamber.

$$\phi_j = \exp\left(\frac{-\|X - C_j\|^2}{2\sigma_j^2}\right). \tag{18}$$

Here, $C_j = \{c_1, c_2, \ldots, c_N\} \in R^N$ represents the centre of the j-th radial basis function ϕ_j, $\|\ \|$ denotes a norm on R^N which is usually considered to be the Euclidean distance and σ is the width parameter related to the radial basis functions ϕ_j. The reason for applying the Gaussian transfer function lies in its ability to adapt well to unseen data without substantially changing the results produced by the input data that have previously been trained (Aharkava, 2010).

Consequently, determining a suitable RBFNN model (Eq. (17)) comprise of a two-step procedure. The first step involves the selection of the basis function centres C_j

(Eq. (18)) and the width parameter σ (Eq. (18)). The second procedure entails calculating the weights values. As explained by Marwala (2013), the output weights and the centres of the basis function can be determined successfully during training by using suitable types of training algorithms including, among others, clustering techniques, gradient descent and least squares algorithm. This study adopted the least squares approach. The least squares technique automatically determines the number of centres insofar as a fixed value of the width parameter of the radial basis function is known. Here, the least squares approach is used as a clustering technique to select centres from a subset of the data set. Detailed description on the least squares algorithm for determining the centres of the radial basis function can be found in (Yih-Jiuan, 1998; Orr, 1996; Chen et al., 1991). After determining the centres, the next step is to calculate the interconnected weights between the hidden and output layers. This is normally accomplished by applying the pseudo-inverse least squares method popularly referred to as Moore–Penrose pseudo inverse (Moore, 1920; Penrose, 1955). The general expression of the weight vector W (Marwala, 2013) is given by Eq. (19) as

$$W_{k\times j} = \left(\phi_{m\times k}\,\phi_{m\times k}^{T} + \lambda\, I_{m\times m}\right)^{-1} \phi^{T} Y_{m\times j}\,, \tag{19}$$

where $\phi_{m\times k}$ is the hidden layer transfer function matrix, $Y_{m\times j}$ is the output matrix with m depicting the training samples, k signifying the number of hidden neurons, I the identity matrix and λ the regularization parameter. Equation (19) reduces to Eq. (20) when there is no regularisation parameter.

$$W_{k\times j} = \left(\phi_{m\times k}\,\phi_{m\times k}^{T}\right)^{-1} \phi^{T} Y_{m\times j}\,. \tag{20}$$

3.4. 2D conformal transformation model

The 2D conformal model consists of four parameters that needed to be determined. The parameters include two translations, a scale factor and rotation. The translation parameters indicate the extent of variation between the origins of the source and target datums. The scale factor creates equal dimension in the reference axes. The rotational parameter depicts the parallelism of the source and target reference axes. The 2D conformal model was applied to transform 2D coordinates from the Leigon 1977 datum to Accra 1929 datum in the Ghana geodetic reference network. The 2D conformal model (Ghilani, 2010) could be expressed in Eq. (21) as

$$\begin{aligned} a\,E_{clark} - b\,N_{clark} + c &= E_{war} \\ b\,E_{clark} + a\,N_{clark} + d &= N_{war} \end{aligned}\,, \tag{21}$$

where $a = \mu\cos\beta$; $b = \mu\sin\beta$; $c = T_x$; $d = T_y$; $\beta = \tan^{-1}\left(\dfrac{b}{a}\right)$; $\mu = \dfrac{a}{\cos\beta}$.

Here a, b, c and d are the unknown transformation parameters to be estimated, (T_x, T_y) are the translations, β is the rotation, μ is the scale factor, (E_{clark}, N_{clark}) and

$(N_{war},\ N_{war})$ are the source and target datum coordinates related to the Leigon 1977 and Accra 1929 datums, respectively. In order to calculate the transformation parameters, Eq. (21) was solved using least squares by expressing it into matrix form as indicated in Eq. (22).

$$BX + V = L, \tag{22}$$

where X is the vector of the unknown transformation parameters to be determined, B is the coefficient matrix of X, V is the residual and L is the vector of the observation. The corresponding matrices of Eq. (22) are given by Eq. (23).

$$B = \begin{bmatrix} E_{clark} & -N_{clark} & 1 & 0 \\ N_{clark} & E_{clark} & 0 & 1 \\ \vdots & \vdots & \vdots & \vdots \\ E_{clark_n} & -N_{clark_n} & 1 & 0 \\ N_{clark_n} & E_{clark_n} & 0 & 1 \end{bmatrix}, \quad X = \begin{bmatrix} a \\ b \\ c \\ d \end{bmatrix}, \quad L = \begin{bmatrix} E_{war} \\ N_{war} \\ \vdots \\ E_{war_n} \\ N_{war_n} \end{bmatrix}, \quad V = \begin{bmatrix} v_{E_{war}} \\ v_{N_{war}} \\ \vdots \\ v_{E_{war_n}} \\ v_{N_{war_n}} \end{bmatrix}. \tag{23}$$

Consequently, X (Eq. (22)) was estimated using Eq. (24).

$$X = (B^T B)^{-1} B^T B. \tag{24}$$

3.5. 2D affine transformation model

The 2D affine model requires the determination of six transformation parameters. The parameters of this model involves two translations of the origin, a rotation about the origin, two scale factors (x- and y-direction) and a lack of orthogonality correction between the x- and y-axes. The 2D affine model was applied to transform 2D coordinates between the two local geodetic datums used in Ghana. The 2D affine model (Sisman, 2014) can be defined in Eq. (25) as

$$\begin{aligned} a\,E_{clark} + b\,N_{clark} + c &= E_{war} \\ d\,E_{clark} + e\,N_{clark} + f &= N_{war} \end{aligned}, \tag{25}$$

where $a = \mu_x \times \cos\alpha$; $b = -\mu_y \times \sin\beta$; $c = T_x$; $d = \mu_x \times \sin\alpha$; $e = \mu_y \times \cos\beta$; $f = T_y$.

Here a, b, c, d, e and f are the unknown transformation parameters to be computed. The rest of the variable terms in Eq. (25) are the same as defined in Eq. (21). To solve for the unknown transformation parameters X, Eq. (25) was simplified into a similar matrix form shown in Eq. (23) and the unknown transformation parameters (X) were then determined using Eq. (24).

3.6. Model construction

The 46 co-located national triangulation points in the two datums which form part of the completed first phase of Ghana GPS reference network (Figure 1) were used in the

ELM, BPNN, RBFNN, 2D conformal, and 2D affine methodology. In order to execute the various methods utilised in this study, the 46 co-located points were partitioned into training and testing. The training data was used to construct the transformation models for the various techniques while the testing data was used to independently assess the competence of the models formed. In this study, 31 co-located points were used for training and the remaining 15 points were used for testing. The training data was carefully selected to cover the entire study area (five regions) as shown in Figure 4. Similarly, the testing points chosen are evenly distributed across the regions under study (Figure 4). The essence is to help provide a better understanding on the efficiency and strength of the various methods when performing 2D coordinate transformation in the study area. In effect, the extent of application for each developed transformation model within the five regions of study (Figure 4) will be clearly known. Figure 4 shows a spatial map of the geographical distributions of the selected training and testing data used in this study.

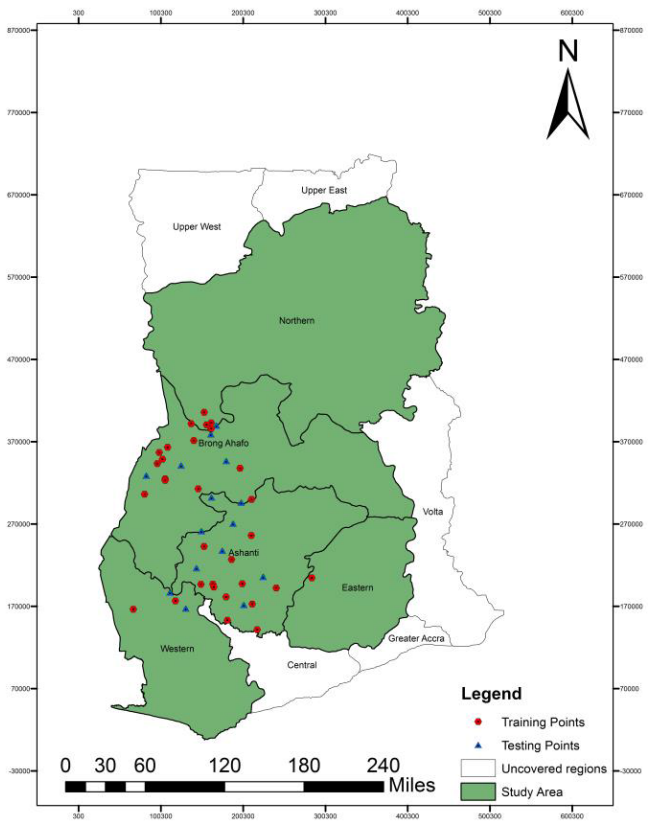

Fig. 4. Selected training and testing data points

Subsequently, the Easting (E) and Northing (N) in the Leigon 1977 datum denoted in this study as (E_{clark}, N_{clark}) was used as the input data while (E_{war}, N_{war}) in the Accra 1929 datum was used as the output data. These were the input and ouput data utilised

to perform the coordinate transformation. The chosen input and output data was then normalized (Mueller and Hemond, 2013) into the interval $[-1,\ 1]$ using Eq. (26).

$$r_i = r_{\min} + \frac{(r_{\max} - r_{\min}) \times (d_i - d_{\min})}{(d_{\max} - d_{\min})}, \tag{26}$$

where r_i represents the normalized data, d_i is the measured coordinate values, while $d_{\min}$ and $d_{\max}$ represents the minimum and maximum value of the measured coordinates with $r_{\max}$ and $r_{\min}$ values set at 1 and -1, respectively.

4. Model adequacy assessments

The quality of the transformation results produced by BPNN, RBFNN, ELM, 2D conformal, and 2D affine model was assessed in conformance with the differences between the measured and the predicted coordinates. To achieve that, the following performance indices (PI) were used: mean squared error (MSE), standard deviation (SD), horizontal positional error (HE), minimum error (min error), maximum error (max error) and average horizontal positional error (MHE). Equations (27) to (31) present their mathematical notations.

$$\text{min error} = \min\left(|D_i - P_i|\right)_{i=1}^{n}, \tag{27}$$

$$\text{max error} = \max\left(|D_i - P_i|\right)_{i=1}^{n}, \tag{28}$$

$$\text{HE} = \sqrt{(E_{D_i} - E_{P_i})^2 + (N_{D_i} - N_{P_i})^2}, \tag{29}$$

$$\text{MHE} = \frac{1}{n}\sum_{i=1}^{n} \text{HE}_i, \tag{30}$$

$$\text{SD} = \sqrt{\frac{1}{n-1}\sum_{i=1}^{n}(e_i - \bar{e})^2}. \tag{31}$$

Here, n is the number of training or testing observation, D and P are the measured and predicted coordinates produced by the various approaches with $i = 1, \ldots,$ n. $\overline{D}$ and $\overline{P}$ is the mean of the measured and predicted coordinates, while e denote the residuals and $\bar{e}$ is the mean of the residuals. $(E_D,\ N_D)$ are the measured coordinates in Easting and Northing and $(E_P,\ N_P)$ are the transformed coordinates produced by the various procedures.

5. Results and discussion

The following sections present the transformation results produced by the various methods applied in this study.

5.1. Transformation parameters estimated

The transformation parameters determined using the 31 co-located points (training data) with their resulting standard deviation (SD) values obtained for the classical 2D affine and 2D conformal models are presented in Tables 1 and 2, respectively. The essence for computing the SD values (Tables 1 and 2) here was to ascertain the precision of the derived transformation parameters by knowing how far the determined parameters vary from it most probable value (mean).

Table 1. 2D affine model transformation parameters from Leigon datum to Accra datum (units in metres)

Parameters	Values	SD
A	1.00001260	2.38E−06
B	1.36E−05	1.36E−06
C	0.5414654	0.6367
D	−5.39E−06	2.38E−06
E	1.00001	1.36E−06
F	−2.3336951	0.6367

Table 2. 2D conformal model transformation parameters from Leigon datum to Accra datum (units in metres)

Parameters	Values	SD
A	1.00001	1.13E−06
B	−0.00001	1.13E−06
C	1.56449	0.37599
D	−1.10457	0.37599

5.2. Soft computing models formed

In the ANNs (BPNN and RBFNN) model formulation, the plane coordinates (E_{clark}, N_{clark}) were used as the input layer data while (E_{war}, N_{war}) was used as the output layer data. In determining the best BPNN and RBFNN structure, the MSE and R values of all the trained models for each training and testing phase were monitored. The model that furnished the least MSE and largest R results in the testing dataset was chosen as the optimum BPNN and RBFNN scheme. The optimum trained RBFNN model consisted of two inputs (E_{clark}, N_{clark}), a single hidden layer with 18 neurons and two

outputs (E_{war}, N_{war}), that is, [2–18–2]. The BPNN, on the other hand, had [2–8–1] for predicting E_{war} output vector and [2–11–1] for the N_{war} output vector. This means that, the optimum BPNN model for predicting the output E_{war} comprised of two inputs with eight hidden neurons while that for the N_{war} consisted of eleven hidden neurons with two inputs. With regards to the ELM, several activation functions were tested in order to select the one that produced the best coordinate transformation results. Upon several trials, the sine activation function expressed in Eq. (32) produced the optimal results. The optimal ELM model structure was [2–24–2]. Thus, two inputs (E_{clark}, N_{clark}) having a single hidden layer with 24 neurons and two outputs (E_{war}, N_{war}), respectively.

$$f(x) = \sin(x). \tag{32}$$

5.3. Test results

After successfully building the trained models, the testing data was employed to assess the veracity of the developed models. This was done by calculating the horizontal positional error (Eq. (29)). The essence was to quantify and provide a better description of how much the transformed coordinates given by BPNN, RBFNN, ELM, 2D conformal and 2D affine deviated from the measured horizontal coordinates.

The computed HE (Eq. (29)) for the various methods are shown in Figure 5 as box-whisker plots. In Figure 5, the central mark is the horizontal error median, the edges of the box is the first and third quartile, and the lower and upper whiskers signify the minimum and maximum error range. The essence of Figure 5 is to provide a graphical rendition of the summary statistics based on the calculated horizontal residuals achieved by each method. In Figure 5, it can be observed that the BPNN, RBFNN and ELM achieved less horizontal positional error variability than the classical 2D affine and 2D

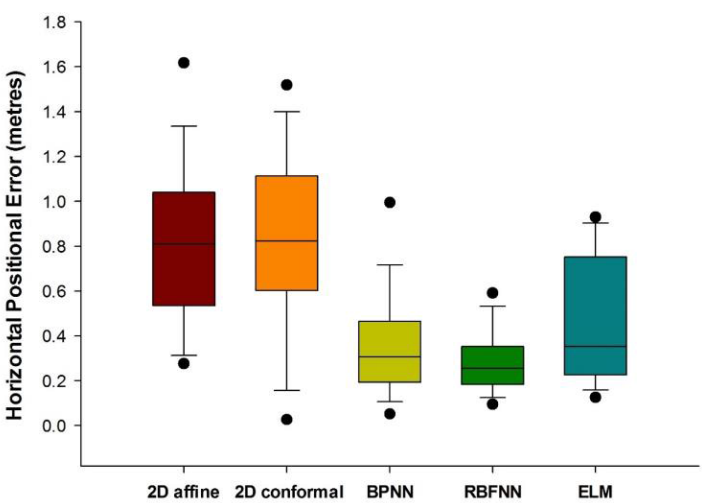

Fig. 5. Horizontal positional error variation based on the testing data

conformal. It is also evident from Fig. 5 that the interquartile range length for the BPNN, RBFNN and ELM is smaller than the 2D affine and 2D conformal models. The error distributions shown in Figure 5 signify that the transformed coordinates produced from the BPNN, RBFNN and ELM vary marginally from the measured positions. These results further suggest that the proposed ELM performed generally well to the widely applied benchmark methods (BPNN and RBFNN) in coordinate transformation.

The strength of BPNN, RBFNN and ELM lies in their ability to learn and adapt to the intrinsic patterns found in the training and testing data sets. Furthermore, the ELM, RBFNN and BPNN adaptive computational strategy gives them more flexibility as compared to the compact nature of the classical transformation equations.

Summary statistics of the horizontal positional errors (Eq. (29)) for the testing data are given in Table 3.

Table 3. Statistics of the total horizontal positional errors for the testing data (units in metres)

Model	MHE	Minimum	Maximum	SD
2D affine	0.799	0.276	1.618	0.357
2D conformal	0.831	0.027	1.519	0.397
BPNN	0.354	0.052	0.995	0.230
RBFNN	0.287	0.095	0.591	0.140
ELM	0.452	0.125	0.930	0.283

In Table 3, the computed MHE (Eq. (30)) results indicate the shifts in average terms between the transformed horizontal positions and the measured data. According to Table 3, the BPNN, RBFNN and ELM model produced an improvement in the average horizontal positional error as compared to the classical techniques. The minimum and maximum results shown in Table 3 quantify the range of horizontal positional errors achieved when the methods were applied in the study area. With respect to the SD values, it can be inferred that the quality of transformation results from BPNN, RBFNN and ELM are far better than the 2D affine and 2D conformal methods.

From a practical point of view, the testing results produced by the BPNN, RBFNN and ELM are logical and related to the legal regulations set by the Ghana Survey and Mapping Division of Lands Commission for cadastral applications and plan production (Yakubu and Kumi-Boateng, 2015). This statement is also buttressed by a comparison between the various transformation precisions (SD values) reported in (Ayer and Fosu, 2008) where 0.354, 0.446 and 0.387 m were achieved by the three-parameter, Bursa–Wolf and Molodensky–Badekas models, respectively. It must be known here that the results presented in (Ayer and Fosu, 2008) is the acceptable standard and applicable transformation results by the Ghana Survey and Mapping Division. Hence, by comparison, the proposed ELM can perform coordinate transformations to cadastral survey accuracies in Ghana. Therefore, the ELM can serve as a reasonable alternative technique for coordinate transformation in the Ghana geodetic reference network.

6. Concluding remarks

As a means to ensure proper surveying practices, coordinate transformation has regularly been seen as a fundamental step for matching data related to different datums onto a common reference surface. Moreover, it is highly essential in developing countries like Ghana where no geocentric datum has been established and only relies on its astro-geodetic datums for geospatial works. Due to the limitation of classical transformation methods which require knowledge of the underlying mathematical function between the co-located coordinates, field practitioners and decision makers must develop alternative tools that can also produce realistic transformation results. Therefore, the main contributions of this study are to evaluate, compare and discuss the capability and applicability of ELM for the first time in coordinate transformation. The obtained results have been compared with the widely used BPNN, RBFNN, 2D affine, and 2D conformal techniques. In conformance with the presented results in this study, it was concluded that the proposed ELM could be used to establish coordinate transformation model that can give satisfactory and reliable transformed coordinates results in the Ghana geodetic reference network. Although comparable transformation results were achieved by the RBFNN, BPNN and ELM in both training and testing stages, the developed ELM method requires lesser computational time compared with the other techniques. Moreover, determining the network architecture of the ELM is simple and straightforward as compared with the BPNN and RBFNN methods respectively. Hence, the proposed ELM is easily applicable. Furthermore, the analyses indicate that the ELM result is appropriate for cadastral survey applications in Ghana. Therefore, the authors suggest that the proposed ELM model can be adapted to perform coordinate transformation in the Ghana geodetic reference network.

Acknowledgments

The authors acknowledge the support from the Ghana Survey and Mapping Division of Lands Commission for making available to us the geodetic triangulation network data of Ghana. We thank the reviewers and the editor for their comments that improved the overall clarity of this paper.

References

Afzali, M., Afzali, A. and Zahedi, G. (2012). The Potential of Artificial Neural Network Technique in Daily and Monthly Ambient Air Temperature Prediction. *International Journal of Environmental Science and Development*, 3 (1), 33–38. DOI: 10.7763/IJESD.2012.V3.183.

Aharkava, L. (2010). Artificial neural networks and self-organization for knowledge extraction. Masters Thesis. Charles University, Faculty of Mathematics and Physics, Prague.

Al-Ruzouq, R. and Dimitrova, P. (2006). Photogrammetric Techniques for Cadastral Map Renewal. TS 90 – GIS and Land Administration Photogrammetric Techniques for Cadastral Map Renewal Shaping the Change XXIII FIG Congress Munich, Germany, October 8–13, 2006.

Ayer, J. (2008). Transformation Models and Procedures for Framework Integration of the Ghana National Geodetic Network. *The Ghana Surveyor*, 1 (2), 52–58.

Ayer, J. and Fosu, C. (2008). Map Coordinate Referencing and the Use of GPS Datasets in Ghana. *Journal of Science and Technology*, 28 (1), 116–127.

Barsi, P. (2001). Performing coordinate transformation by artificial neural network. *Allgemeine Vermessungs-Nachrichten*, 4, 134–137.

Bishop, C.M. (1995). *Neural networks for pattern recognition*. Oxford, UK: Oxford University Press.

Broomhead, D.S. and Lowe, D. (1988). Multivariate functional interpolation and adaptive networks. *Complex Systems*, 2, 321–355.

Chang, N.B., Han, M., Yao, W., Chen, L.C. and Xu, S. (2010). Change detection of land use and land cover in an urban region with SPOT-5 images and partial Lanczos extreme learning machine. *Journal of Applied Remote Sensing*, 4 (1), 11–15. DOI: 10.1117/1.3518096.

Chen, S., Cowan, C.F.N. and Grant, P.M. (1991). Orthogonal Least Squares Learning Algorithm for Radial Basis Functions Networks. *IEEE Transaction on Neural Networks*, 2 (2), 302–309. DOI: 10.1109/72.80341.

Deakin, R.E. (2007). Coordinate transformations for cadastral surveying. School of Mathematical and Geospatial Sciences, RMIT University, 1–34.

Deo, R.C. and Şahin, M. (2016). An extreme learning machine model for the simulation of monthly mean streamflow water level in eastern Queensland. *Environmental Monitoring and Assessment*, 188 (2), 1–24. DOI: 10.1007/s10661-016-5094-9.

Deo, R.C., Tiwari, M.K., Adamowski, J.F. and Quilty, J.M. (2017). Forecasting effective drought index using a wavelet extreme learning machine (W-ELM) model. *Stochastic Environmental Research and Risk Assessment*, 31 (5), 1211–1240. DOI: 10.1007/s00477-016-1265-z.

Dönmez, Ş.Ö. and Tunc, A. (2016). Transformation methods for using combination of remotely sensed data and cadastral maps. The International Archives of the Photogrammetry, Remote Sensing and Spatial Information Sciences, Volume XLI-B4, 2016 XXIII ISPRS Congress, 12–19 July 2016, Prague, Czech Republic, 587–589. DOI: 10.5194/isprsarchives-XLI-B4-587-2016.

Dzidefo, A. (2011). Determination of transformation parameters between the World Geodetic System 1984 and the Ghana geodetic network. Masters Thesis, Department of Civil and Geomatic Engineering, KNUST, Kumasi, Ghana.

ElSayed, M.S. and Ali, A.H. (2016). Performance Evaluation of Applying Fuzzy Multiple Regression Model to TLS in the Geodetic Coordinate Transformation. *American Scientific Research Journal for Engineering, Technology, and Sciences*, 25 (1), 36–50.

Fosu, C., Poku-Gyamfi, Y. and Hein, W.G. (2006). Global Navigation Satellite System (GNSS) – A Utility for Sustainable Development in Africa. 5th FIG Regional Conference on Promoting Land Administration and Good Governance, Workshop – AFREF I, Accra, Ghana, 1–12.

Fotiou, A. and Kaltsikis, C.J. (2016). Computationally efficient methods and solutions with least squares similarity transformation models. https://www.researchgate.net/profile/Aristeidis_Fotiou/publication/309732142_Computationally_efficient_methods_and_solutions_with_least_squares_similarity_transformation_models/links/58204df808ae12715afbb0c6/Computationally-efficient-methods-and-solutions-with-least-squares-similarity-transformation-models.pdf. Accessed 2 January 2018.

Ghilani, C.D. (2010). Adjustment Computations: Spatial Data Analysis, 5th edition, John Wiley & Sons Inc., Hoboken, New Jersey.

Gil, J. and Mrówczyńska, M. (2010). Methods of Artificial Intelligence used for Transforming a System of Coordinates. *Geodetski list*, 66 (4), 321–336.

Gullu, M. (2010). Coordinate Transformation by Radial Basis Function Neural Network. *Scientific Research and Essays*, 5, 3141–3146.

Gullu, M., Yilmaz, M., Yilmaz, I. and Turgut, B. (2011). Datum transformation by artificial neural networks for geographic information systems applications. International Symposium on Environmental Protection and Planning: Geographic Information Systems (GIS) and Remote Sensing (RS) Applications (ISEPP) Izmir – Turkey, 13–19.

Hao, Y. and Wilamowski, B.M. (2011). Levenberg–marquardt training. Industrial Electronic Handbook, vol. 5 Intelligent Systems, 2nd Edition, Chapter 12, 1–15, CRC Press.

Hornik, K., Stinchcombe, M. and White, H. (1989). Multilayer feed forward networks are universal approximators. *Neural Networks*, 2, 359–366.

Huang, F., Huang, J., Jiang, S. and Zhou, C. (2017). Landslide displacement prediction based on multivariate chaotic model and extreme learning machine. *Engineering Geology*, 218, 173–186. DOI: 10.1016/j.enggeo.2017.01.016.

Huang, G., Huang, G.B., Song, S. and You, K. (2015). Trends in extreme learning machines: A review. *Neural Networks*, 61, 32–48. DOI: 10.1016/j.neunet.2014.10.001.

Huang, G.B. and Babri, H.A. (1998). Upper bounds on the number of hidden neurons in feedforward networks with arbitrary bounded nonlinear activation functions. *IEEE Transaction on Neural Networks*, 9 (1), 224–229. DOI: 10.1109/72.655045.

Huang, G.B., Chen, L.and Siew, C.K. (2006b). Universal approximation using incremental constructive feedforward networks with random hidden nodes. *IEEE Transaction on Neural Networks*, 17 (4), 879–892. DOI: 10.1109/TNN.2006.875977.

Huang, G.B., Zhu, Q.Y. and Siew, C.K. (2006a). Extreme learning machine: Theory and applications. *Neurocomputing*, 70, 489–501. DOI: 10.1016/j.neucom.2005.12.126.

Konakoğlu, B., Cakir L. and Gökalp, E. (2016). 2D coordinates transformation using artificial neural networks. Geo Advances 2016: ISPRS Workshop on Multi-dimensional & Multi-scale Spatial Data Modeling, At Mimar Sinan Fine Arts University/Istanbul, Volume XLII-2/W1: 3rd International GeoAdvances Workshop. DOI: 10.5194/isprs-archives-XLII-2-W1-183-2016.

Konakoğlu B. and Gökalp, E. (2016). A Study on 2D similarity transformation using multilayer perceptron neural networks and a performance comparison with conventional and robust outlier detection methods. *Acta Montanistica Slovaca*, 21 (4), 324–332.

Kotzev, V. (2013). Consultancy service for the selection of a new projection system for Ghana. Draft Final Reports, World Bank Second Land Administration Project (LAP-2), Ghana.

Kumi-Boateng, B. and Ziggah, Y.Y. (2017). Horizontal coordinate transformation using artificial neural network technology – A case study of Ghana geodetic reference network. *Journal of Geomatics*, 11 (1), 1–11.

Lao-Sheng, L. and Yi-Jin, W. (2006). A study on cadastral coordinate transformation using artificial neural network. Proceedings of the 27th Asian Conference on Remote Sensing, Ulaanbaatar, Mongolia.

Lazarevska, E. (2016). Wind speed prediction with extreme learning machine. 2016 IEEE 8th International Conference on Intelligent Systems (IS), Sofia, 154–159. DOI: 10.1109/IS.2016.7737415.

Lei, Y., Zhao, D. and Cai, H. (2015). Prediction of length-of-day using extreme learning machine. *Geodesy and Geodynamics*, 6 (2), 151–159. DOI: 10.1016/j.geog.2014.12.007.

Lian, C., Zeng, Z., Yao, W. and Tang, H. (2014). Extreme learning machine for the displacement prediction of landslide under rainfall and reservoir level. *Stochastic environmental research and risk assessment*, 28(8), 1957–1972. DOI: 10.1007/s00477-014-0875-6.

Marwala, T. (2013). Economic Modeling Using Artificial Intelligence Methods. Springer-Verlag London.

Mihalache, R.M. (2012). Coordinate transformation for integrating map information in the new geocentric European system using artificial neural networks. *GeoCAD*, 1–9.

Mohammadi, K., Shamshirband, S., Motamedi, S., Petković, D., Hashim, R. and Gocic, M. (2015). Extreme learning machine based prediction of daily dew point temperature. *Computers and Electronics in Agriculture*, 117, 214–225. DOI: 10.1016/j.compag.2015.08.008.

Moore, E.H. (1920). On the reciprocal of the general algebraic matrix. *Bulletin of the American Math Society*, 26, 394–395.

Mugnier, J.C. (2000). OGP-coordinate conversions and transformations including formulae, COLUMN, Grids and Datums. The Republic of Ghana. *Photogrammetric Engineering and Remote Sensing*, 695–697.

Muller, V.A. and Hemond, F.H. (2013). Extended artificial neural networks: incorporation of a priori chemical knowledge enables use of ion selective electrodes for in-situ measurement of ions at environmentally relevant levels. *Talanta*, 117, 112–118. DOI: 10.1016/j.talanta.2013.08.045.

Orr, M.J.L. (2009). Introduction to Radial Basis Function Networks. Center for Cognitive Science, Edinburgh University, Scotland, UK.

Pal, M. (2009). Extreme-learning-machine-based land cover classification. *International Journal of Remote Sensing*, 30 (14), 3835–3841. DOI: 10.1080/01431160902788636.

Penrose, R. (1955) A generalized inverse for matrices. *In Mathematical proceedings of the Cambridge Philosophical Society*, 51 (3), 406–413. DOI: 10.1017/S0305004100030401.

Poku-Gyamfi, Y. (2009). Establishment of GPS Reference Network in Ghana. PhD Dissertation, Universitat der Bundeswehr Munchen, Germany.

Rumelhart, D.E., McClelland, J.L. and PDP Research Group. (1986). Parallel Distributed Processing: Explorations in the Microstructure of Cognition. MIT Press, Cambridge, Massachusetts, USA.

Sisman, Y. (2014). Coordinate transformation of cadastral maps using different adjustment methods. *Journal of Chinese Institute of Engineers*, 37 (7), 869–882. DOI: 10.1080/02533839.2014.888800.

Swadi, G. (2010). A study of prediction in seabed mapping. PhD Dissertation. University of Wales Institute, Cardiff, Wales.

Tierra, A. and Romero, R. (2014). Planes Coordinates Transformation between PSAD56 to SIRGAS using a Multilayer Artificial Neural Network. *Geodesy and Cartography*, 63, 199–209. DOI: 10.2478/geocart-2014-0014.

Tierra, A., Dalazoana, R. and De Freitas, S. (2008). Using an Artificial Neural Network to Improve the Transformation of Coordinates between Classical Geodetic Reference Frames. *Computers & Geosciences*, 34, 81–189. DOI: 10.1016/j.cageo.2007.03.011.

Tierra, A.R., De Freitas, S.R.C. and Guevara, P.M. (2009). Using an Artificial Neural Network to Transformation of Coordinates from PSAD56 to SIRGAS95. Geodetic Reference Frames, International Association of Geodesy Symposia, 134, 173–178. DOI: 10.1007/978-3-642-00860-3_27.

Tiwari, M., Adamowski, J. and Adamowski, K. (2016). Water demand forecasting using extreme learning machines. *Journal of Water and Land Development*, 28 (1), 37–52. DOI: 10.1515/jwld-2016-0004.

Turgut, B. (2010). A Back-Propagation Artificial Neural Network Approach for Three-Dimensional Coordinate Transformation. *Science and Research Essay*, 5, 3330–3335.

Wu, C.H., Chou, H.J. and Su, W.H. (2008). Direct transformation of coordinates for GPS positioning using the techniques of genetic programming and symbolic regression. *Engineering Applications of Artificial Intelligence*, 21 (8), 1347–1359. DOI: 10.1016/j.engappai.2008.02.001.

Yakubu, I. and Kumi-Boateng, B. (2015). Ramification of datum and ellipsoidal parameters on post processed differential global positioning system (DGPS) data – A case study. *Ghana Mining Journal*, 15, 1–9.

Yih-Jiuan, W. (1998). Exchange rate forecasting: an application of radial basis function neural networks. Iowa State University, USA.

Yilmaz, I. and Gullu, M. (2012). Georeferencing of Historical Maps using back propagation artificial neural network. *Experimental Techniques*, 3 (5), 15–19. DOI: 10.1111/j.1747-1567.2010.00694.x.

Yonaba, H., Anctil, F. and Fortin, V. (2010). Comparing sigmoid transfer functions for neural network multistep ahead stream flow forecasting. *Journal of Hydrologic Engineering*, 15(4), 275–283. DOI: 10.1061/(ASCE)HE.1943-5584.0000188.

Zaletnyik, P. (2004). Coordinate Transformation with Neural Networks and with Polynomials in Hungary. International Symposium on Modern Technologies, Education and Professional Practice in Geodesy and Related Fields, Sofia, Bulgaria, 471–479.

Zhang, S., Zhang, K. and Liu, P. (2016). Total Least-Squares Estimation for 2D Affine Coordinate Transformation with Constraints on Physical Parameters. *Journal of Surveying Engineering*, 142 (3), 04016009-1-04016009-5. DOI: 10.1061/(ASCE)SU.1943-5428.0000180.

Zhang, Y., Ding, S., Xu, X., Zhao, H. and Xing, W. (2013). An Algorithm Research for Prediction of Extreme Learning Machines Based on Rough Sets. *Journal of Computers*, 8 (5), 1335–1342. DOI: 10.4304/jcp.8.5.1335-1342.

Ziggah, Y.Y., Youjian, H., Tierra, A., Konaté, A.A. and Hui, Z. (2016). Performance evaluation of artificial neural networks for planimetric coordinate transformation — a case study, Ghana. *Arabian Journal of Geosciences*, 9 (17), 1–16. DOI: 10.1007/s12517-016-2729-7.

Zounemat-Kermani, M. (2012). Hydrometeorological parameters in prediction of soil temperature by means of artificial neural network: Case study in Wyoming. *Journal of Hydrologic Engineering*, 18 (6), 707–718. DOI: 10.1061/(ASCE)HE.1943-5584.0000666.